Electronic supplementary materials *Mendeleev Commun.*, 2020, **30**, 516-518

The effect of N-substituent on the relative thermodynamic stability of unionized and zwitterionic forms of α-diphenylphosphino-α-amino acids

Olga S. Soficheva, Alina A. Nesterova, Alexey B. Dobrynin, Ekaterina M. Zueva, Joachim W. Heinicke, Oleg G. Sinyashin and Dmitry G. Yakhvarov

I. General procedures

All manipulations and reactions with air-sensitive compounds were conducted under nitrogen using Schlenk techniques. Solvents were dried by standard methods and freshly distilled before use. NMR tubes of samples repeatedly measured over several days were closed by ground glass joints or sealed off to avoid slow oxidation by air diffusing through the usual plastic caps. Commercial diphenylphosphine, methyl 2-aminobenzoate, and glyoxylic acid monohydrate (Sigma-Aldrich) were used as purchased. Glyoxylic acid monohydrate was dissolved in diethyl ether using an ultrasonic bath. α-Diphenylphosphino-*N*-(*tert*-butyl)glycine (**1**)[S1], α-diphenylphosphino-*N*-(*p*-tolyl)glycine (**2a**)[S2], α-diphenylphosphino-*N*-(quinolin-3-yl)glycine (**2b**)[S3], α-diphenylphosphino-*N*-(pyrazin-2-yl)glycine (**2c**)[S4], α-diphenylphosphino-*N*-[2,5-bis(methoxycarbonyl)phenyl]glycine (**2d**)[S5] were obtained and characterized as reported.

NMR spectra were recorded with a multinuclear Bruker ARX400 FT-NMR spectrometer at 400 (^{1}H), 150 (^{13}C) and 160 (^{31}P) MHz in DMF-d$_7$. Chemical shifts (δ) are given in ppm and referred to tetramethylsilane for ^{1}H and ^{13}C NMR and to H_3PO_4 (85%) for ^{31}P NMR. Elemental analyses were determined with a CHNS-932 analyzer from LECO (standard conditions).

X-ray diffraction analysis was performed on automatic diffractometer Bruker Kappa Apex II CCD diffractometer using graphite monochromated Mo-Kα (0.71073 Å) radiation and ω-scan rotation. Data collection: images were indexed, integrated, and scaled using the APEX2[S6] data reduction package and corrected for absorption using SADABS.[S7] The structure of α-diphenylphosphino-*N*-(2-methoxycarbonylphenyl)glycine (**2e**) was solved by the direct methods and refined using SHELX.[S8] Non-hydrogen atoms were refined anisotropically. The hydrogen atoms of the OH- and NH-groups were revealed by means of the difference electron density maps and refined in the isotropic approximation. Other hydrogen atoms were calculated at idealized positions and refined as riding atoms. All calculations were performed using WinGX.[S9] Intermolecular interactions were analyzed using the program PLATON.[S10] All the figures were produced by the MERCURY program.[S11]

CCDC 1996686 contains the supplementary crystallographic data for this paper. These data can be obtained free of charge from The Cambridge Crystallographic Data Centre *via* http://www.ccdc.cam.ac.uk.

Quantum-chemical calculations (geometry optimizations and Gibbs free energy calculations) were done within the spin-restricted density functional theory (DFT) framework using the Gaussian 09 package.[S12] The computational procedure employs the B3LYP functional in conjunction with the all-electron def2-TZVP basis set for all atoms. Solvent effects were accounted for implicitly using the self-consistent reaction field (SCRF) and the solvation model density (SMD) continuum models with ε = 32.613 (MeOH) and 4.240 (Et_2O).

II. Crystal structure of known compounds

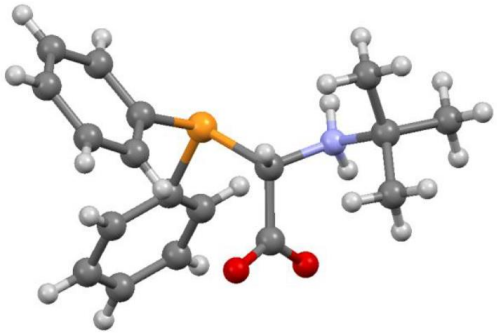

1

Figure S1. The solid-state molecular structure of α-diphenylphosphino-*N*-(*tert*-butyl)glycine (**1**).[S1]

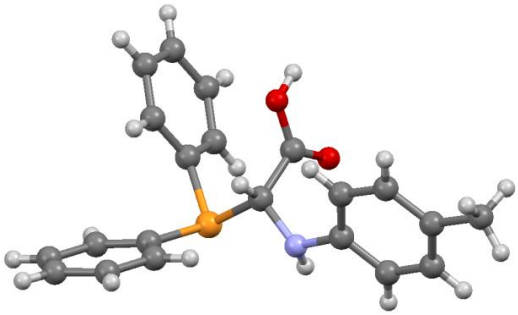

2a

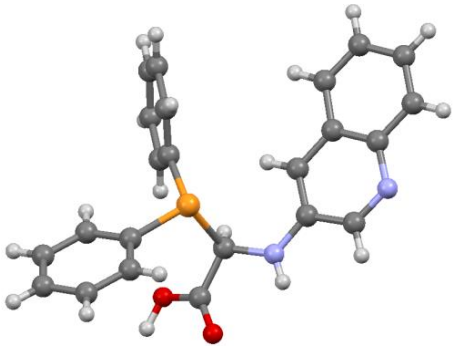

2b

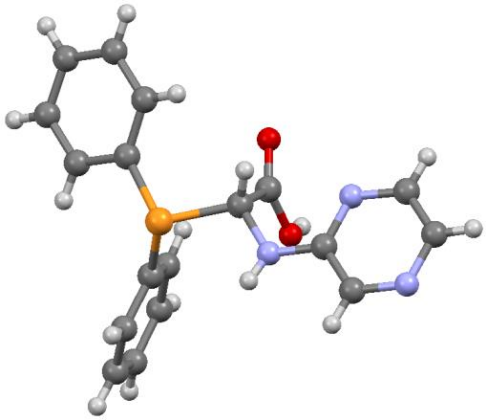

2c

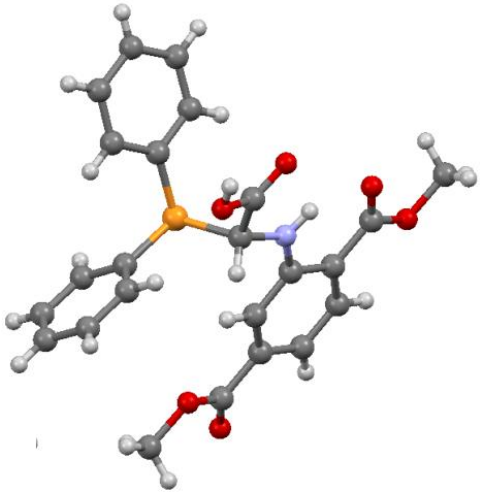

2d

Figure S2. The solid-state molecular structures of α-diphenylphosphino-*N*-(*p*-tolyl)glycine (**2a**),[S2] α-diphenylphosphino-*N*-(quinolin-3-yl)glycine (**2b**),[S3] α-diphenylphosphino-*N*-(pyrazin-2-yl)glycine (**2c**)[S4] and α-diphenylphosphino-*N*-[2,5-bis(methoxycarbonyl)phenyl]glycine (**2d**).[S5]

III. Synthesis and characterization

*Preparation of α-diphenylphosphino-N-(2-methoxycarbonylphenyl)glycine (**2e**).* Glyoxylic acid hydrate (0.273 g, 2.87 mmol) was dissolved in methanol (10 ml), and this solution was added to a mixture containing diphenylphosphine (0.535 g, 2.87 mmol) and methyl 2-aminobenzoate (0.433 g, 2.87 mmol) in methanol (15 ml). The mixture was stirred at room temperature for 5 hours. The formed white precipitate was filtered off, washed with diethyl ether and dried *in vacuo* to afford product **2e** (1.05 g, 93%) as a white powder.

^{1}H-NMR (DMF-d_7): δ = 3.84 (s, 2-OCH_3), 4.22 (br d, $^{2}J_{PH}$ = 5 Hz, PCH), 5.36 (d, ^{3}J = 8.4 Hz, 1 H, NH), 6.72 (td, ^{3}J = 6.1, ^{4}J = 1.0 Hz, 1 H, 4'-H), 6.99 (d, ^{3}J = 8.5 Hz, 1 H, 6'-H), 7.44-7.49 (m, 6 H, Ph), 7.61-7.66 (m, 2 H, Ph), 7.70-7.75 (m, 2 H, Ph), 7.99(dd, ^{3}J = 8.1, ^{4}J = 1.6 Hz, 1 H, 3'-H), 8.43 (dd, ^{3}J = 8.5, ^{4}J = 2.3 Hz, 1 H, 5'-H) ppm (Fig. S3).

^{13}C{^{1}H} NMR (DMF-d_7): δ = 51.43 (s, 2-OMe), 56.28 (d, ^{2}J = 23.05 Hz, NCH), 111.09 (s, 2'-C_q), 112.69 (s, 6'-CH), 115.96 (s, 4'-CH), 128.62 (d, ^{3}J = 6.84 Hz, 2 *m*-*C*H), 128.80 (d, ^{3}J = 6.14 Hz, 2 *m*-*C*H), 129.49 (s, *p*-CH), 129.76 (s, *p*-CH), 131.60 (s, 3'- or 5'-CH), 133.56 (d, ^{2}J = 19.9 Hz, 2 *o*-CH), 134.06 (d, ^{2}J = 20.6 Hz, 2 *o*-*C*H), 134.81 (superimposed s, 5'- or 3'-CH), 134.86 (d, ^{1}J = 15.97 Hz, 2 *i*-C_q), 149.92 (s, NC_q-1'), 171.68 (d, $^{2}J_{PC}$ = 7.8 Hz, COOH) ppm (Fig. S4).

^{31}P{^{1}H} NMR (DMF-d_7): δ = 1.95 ppm (Fig. S5).

IR (KBr): ν = 3310 (wm), 3066 (wm), 3002 (wm), 2943 (wm), 2841 (w), 2615 (w), 1888 (st), 1692 (vst), 1577 (wm), 1508 (st), 1438 (st), 1321 (st), 1238 (m), 1160 (vst), 1079 (m) cm^{-1}.

Calc. for $C_{22}H_{20}NO_4P$ (M = 392.37 g × mol^{-1}): C, 67.34, H, 4.88, N, 3.57; found: C, 67.40, H, 4.98, N, 3.45.

*Crystal structure analysis of α-diphenylphosphino-N-(2-methoxycarbonylphenyl)glycine (**2e**).*

$C_{22}H_{20}NO_4P$ (M = 393.36), triclinic, space group P-1 at 294 K: a = 8.2651(7), b = 9.7114(8), c = 13.1428(9) Å, α = 75.352(3), β = 88.534(3), γ = 68.600(3)°, V = 947.66(13) $Å^3$, Z = 2, d_{calc} = 1.378 g cm^{-3}; μ(Mo-Kα) = 0.174 mm^{-1}; F(000) = 412. Total of 12747 reflections were collected (4126 independent reflections with $\theta < 27°$, R_{int} = 0.065) and used in the refinement, which converged to wR_2 = 0.1357, GOOF = 0.83 for all independent reflections [R_1 = 0.0390 was calculated for 3359 reflections with $I \geq 2\sigma(I)$].

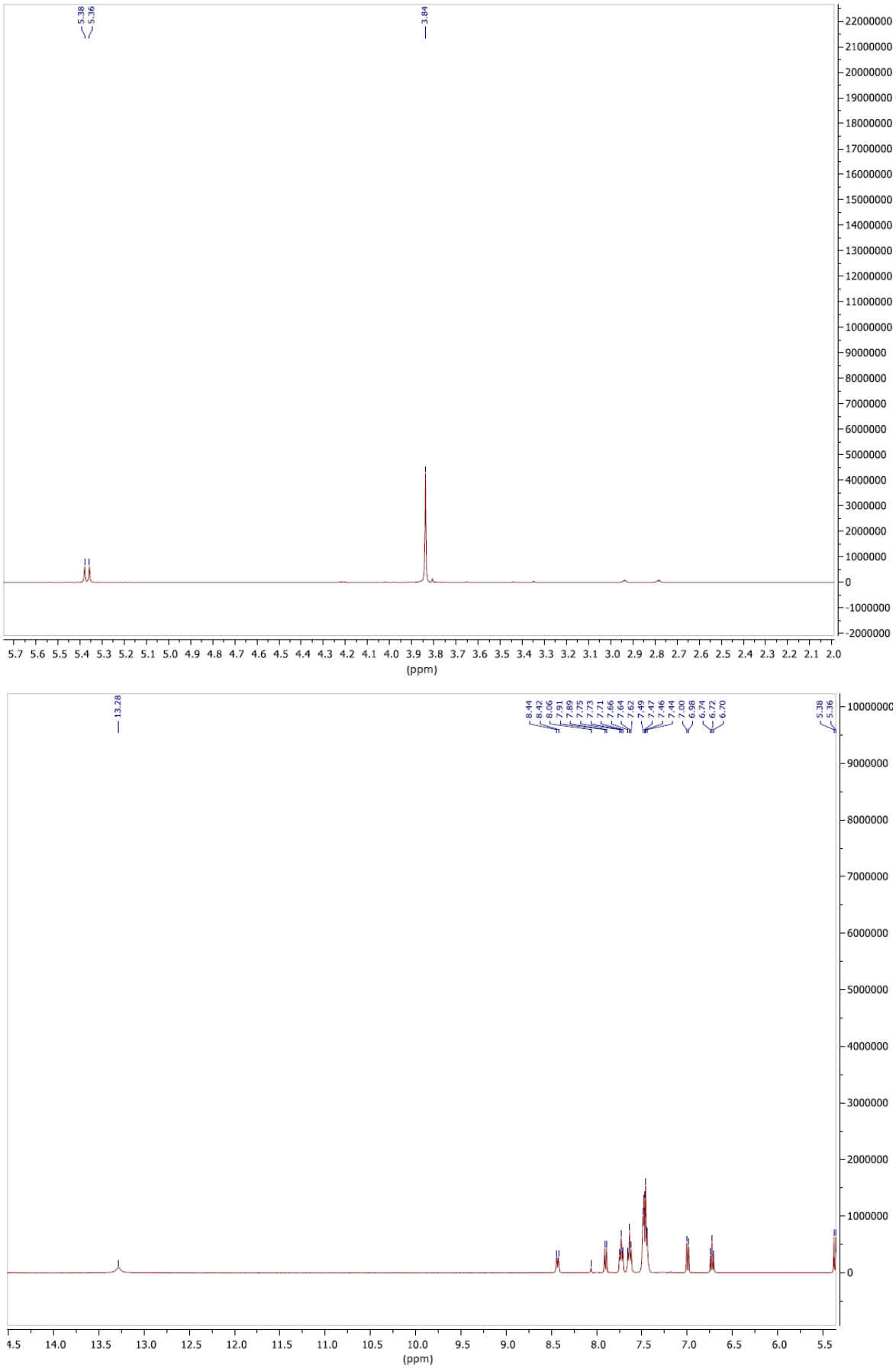

Figure S3. The alkyl and aryl ranges of ^{1}H NMR spectrum of α-diphenylphosphino-*N*-(2-methoxycarbonylphenyl)glycine (**2e**).

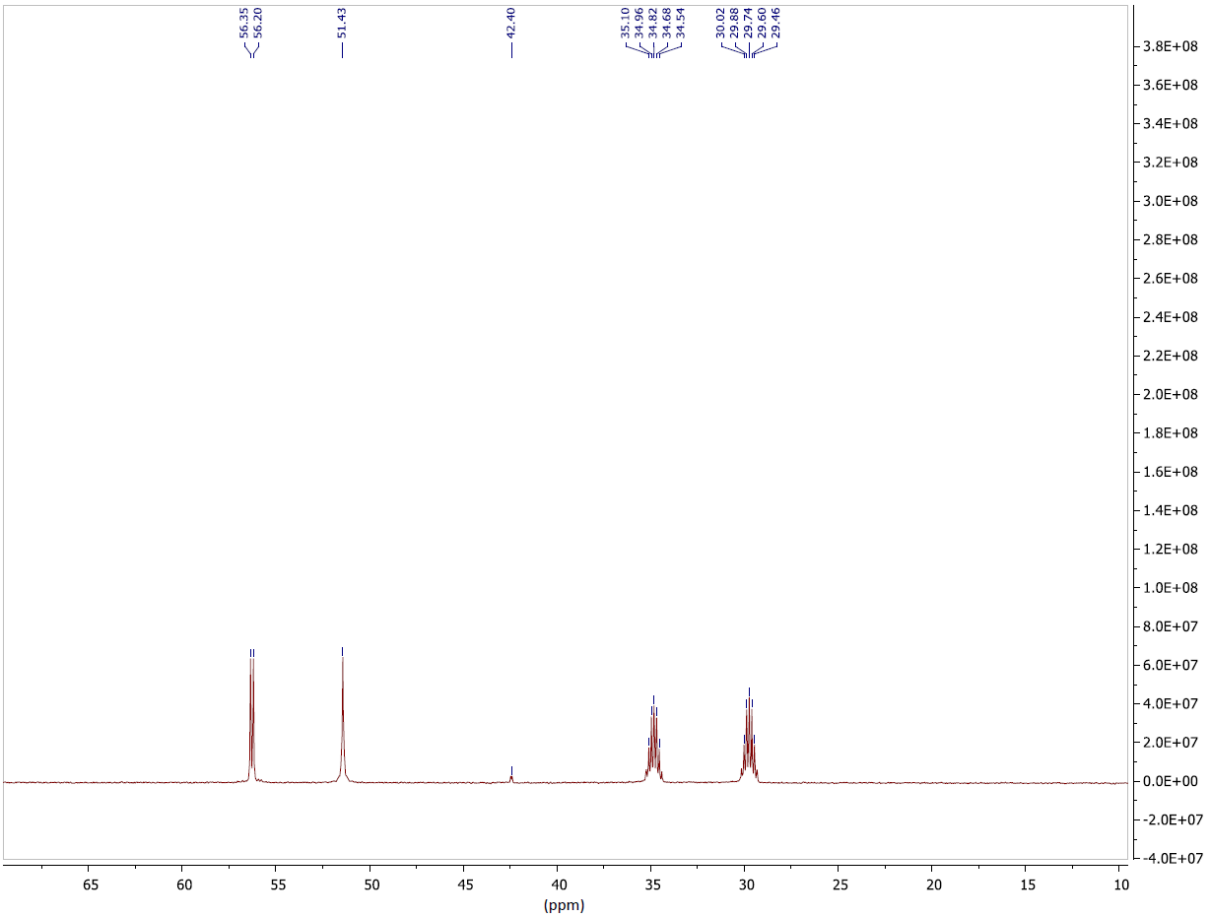
56.35
56.20
51.43
42.40
35.10
34.96
34.82
34.68
34.54
30.02
29.88
29.74
29.60
29.46
3.8E+08
3.6E+08
3.4E+08
3.2E+08
3.0E+08
2.8E+08
2.6E+08
2.4E+08
2.2E+08
2.0E+08
1.8E+08
1.6E+08
1.4E+08
1.2E+08
1.0E+08
8.0E+07
6.0E+07
4.0E+07
2.0E+07
0.0E+00
-2.0E+07
-4.0E+07
65
60
55
50
45
40
35
30
25
20
15
10
(ppm)

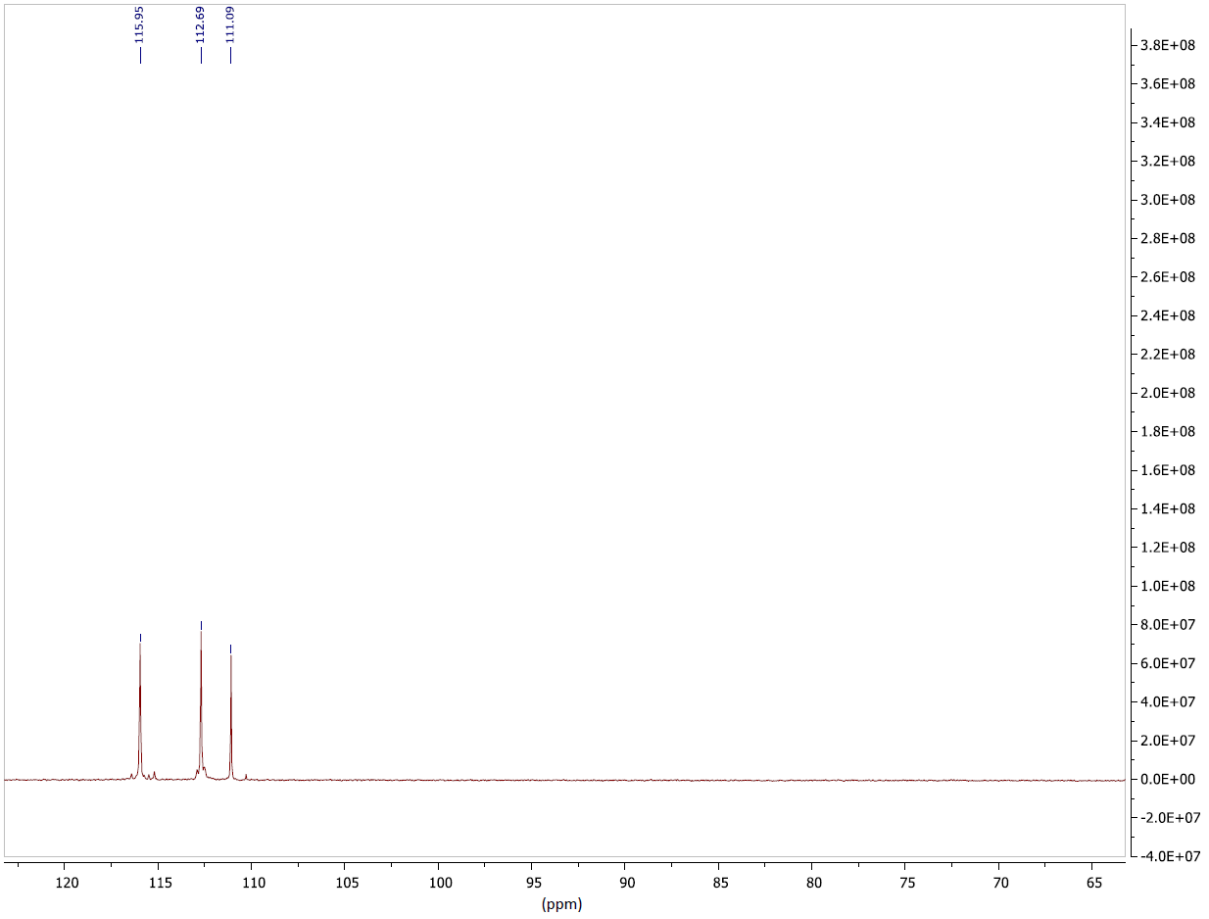
115.95
112.69
111.09
3.8E+08
3.6E+08
3.4E+08
3.2E+08
3.0E+08
2.8E+08
2.6E+08
2.4E+08
2.2E+08
2.0E+08
1.8E+08
1.6E+08
1.4E+08
1.2E+08
1.0E+08
8.0E+07
6.0E+07
4.0E+07
2.0E+07
0.0E+00
-2.0E+07
-4.0E+07
120
115
110
105
100
95
90
85
80
75
70
65
(ppm)

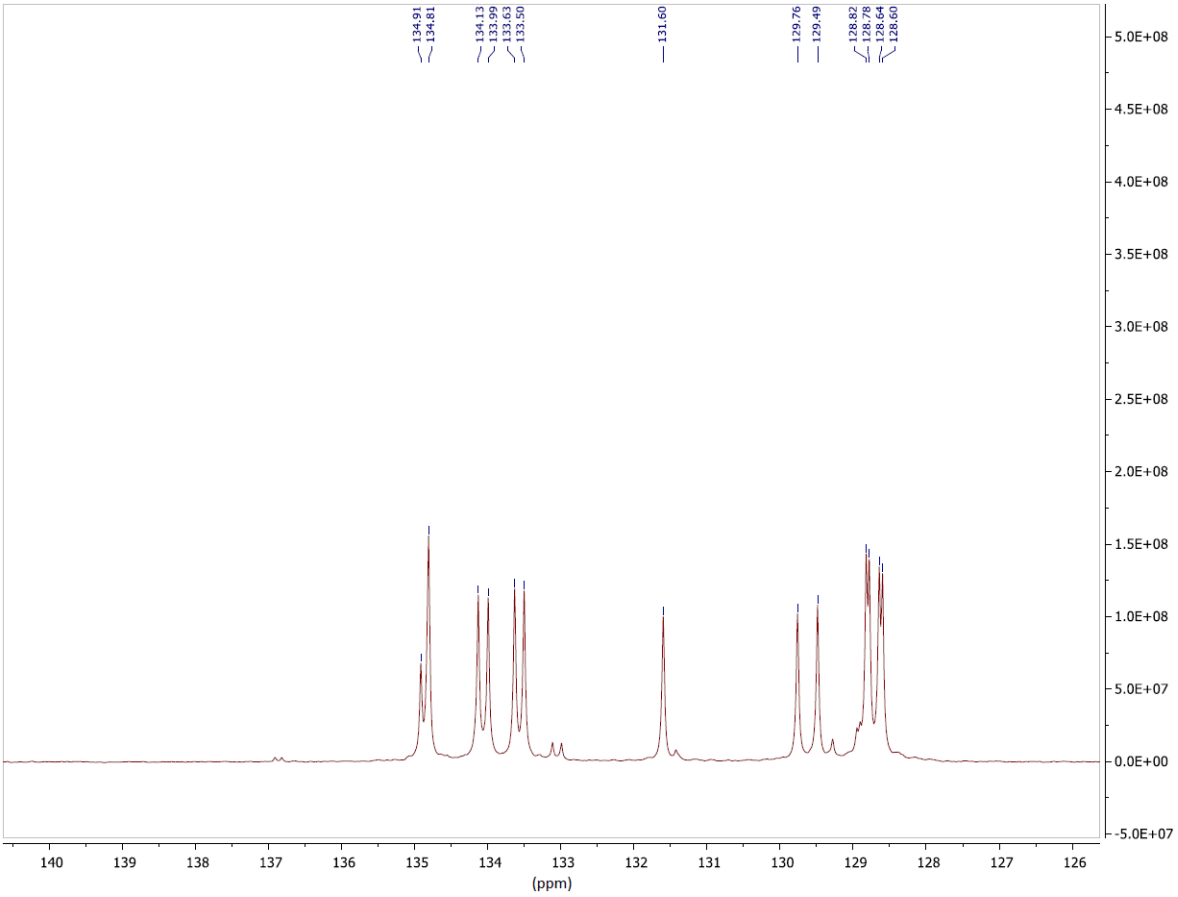

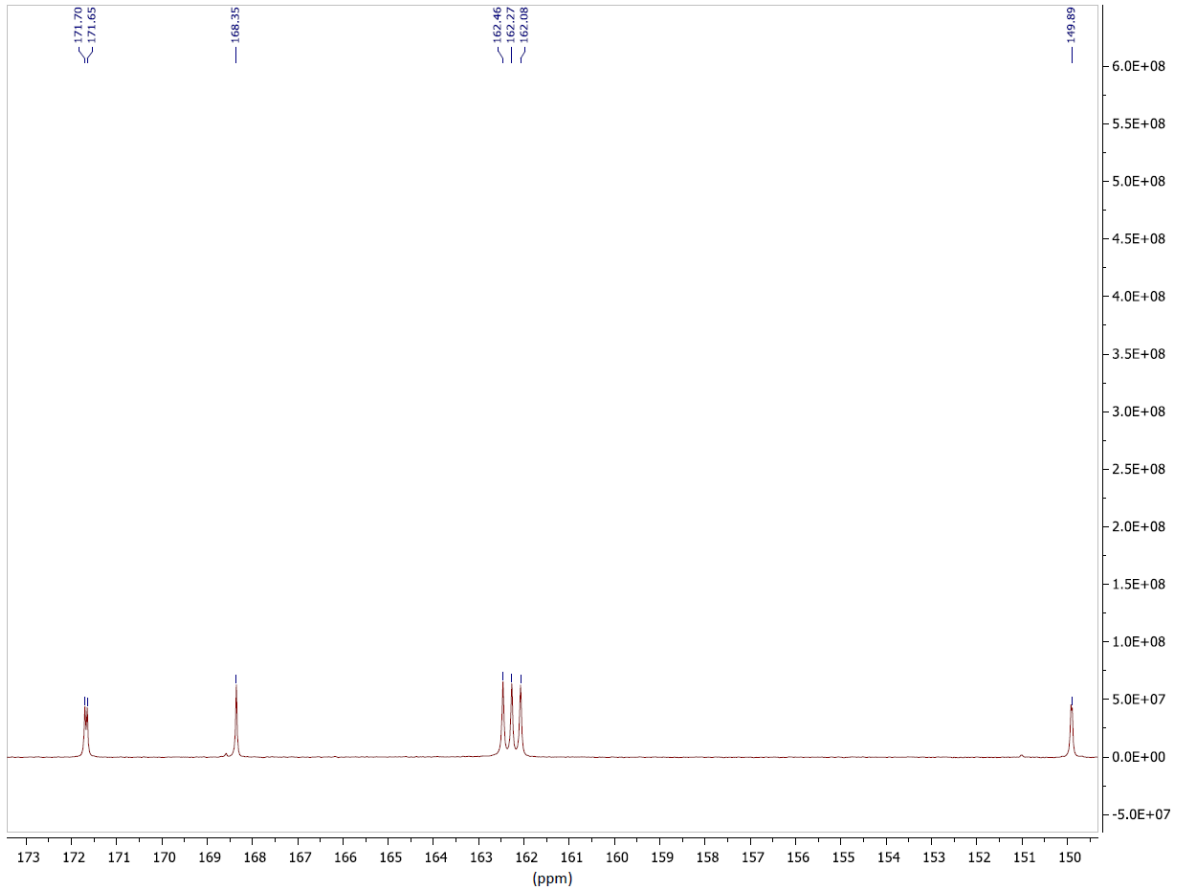

Figure S4. ^{13}C NMR spectrum of α-diphenylphosphino-*N*-(2-methoxycarbonylphenyl)glycine (**2e**).

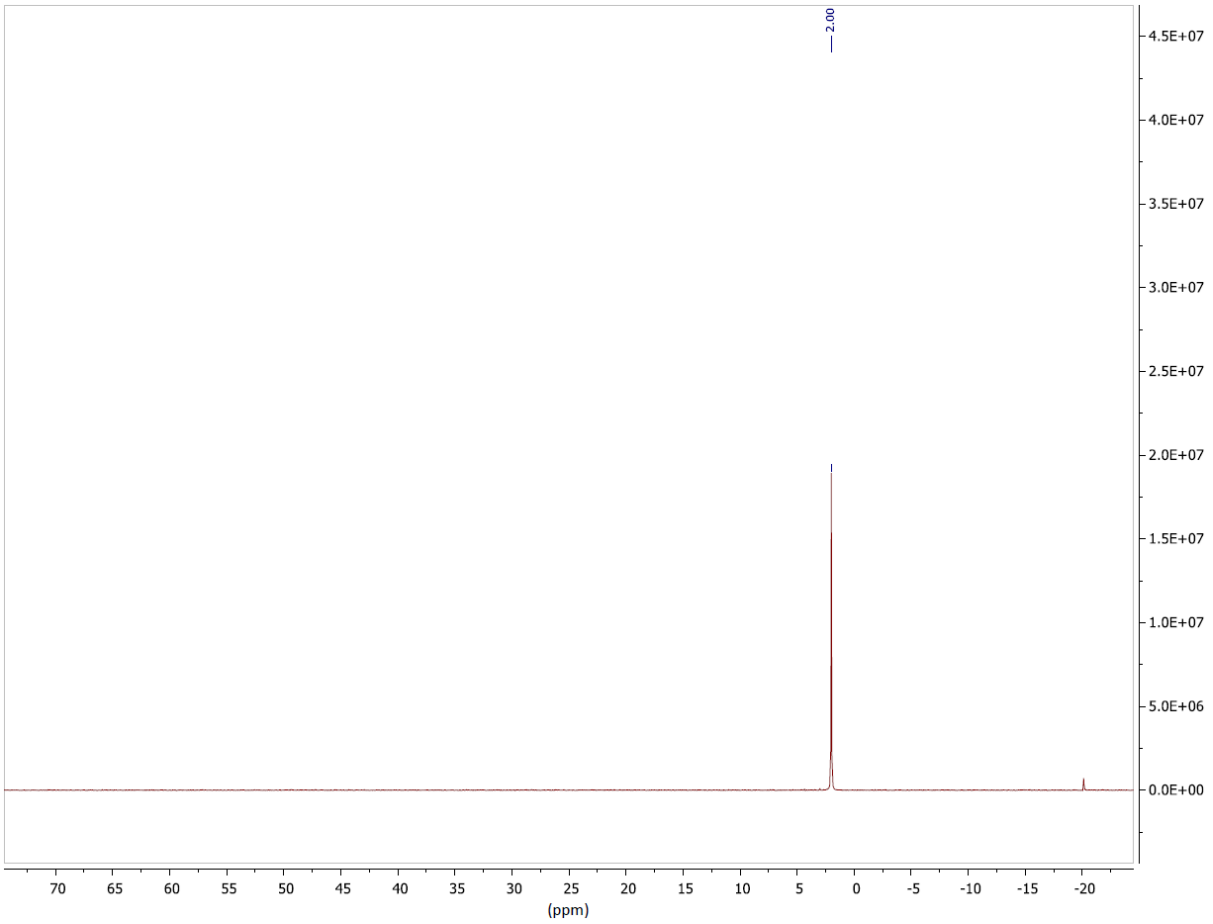

Figure S5. ^{31}P NMR spectrum of α-diphenylphosphino-*N*-(2-methoxycarbonylphenyl)glycine (**2e**).

IV. Quantum-chemical calculations

To get an insight into the influence of the aromatic substituent at the nitrogen atom, we performed a quantum-chemical analysis of molecular structures and the relative thermodynamic stability of unionized (UIF) and zwitterionic (ZIF) forms of **2a-e** (Tables S1–S6). The same analysis was also performed for **1** for comparison (Tables S7 and S8).

Analysis of the X-ray diffraction data for **2a-e** showed that the unionized form of these conformationally flexible compounds can be found in various conformations. Based on these data, the following conformational series was proposed: I-a, I-b, IIA-a, IIA-b, IIB-a, IIB-b. Herein, I and II are conformations associated with the rotation about the C(H)–N bond. Symbols a and b indicate different conformers resulting from the rotation about the P–C(H) bond. For II, we also considered an additional degree of conformational freedom associated with the rotation about the C(H)–$C_{carboxyl}$ bond (A and B conformers). Molecular structures optimized for all these unionized conformers and the corresponding zwitterionic counterparts are shown in Tables S1–S5 separately for each compound (**2a-e**, respectively). The values of the Gibbs free energies (G^0_{UIF} and G^0_{ZIF}) and their difference (ΔG^0) are

given in Table S6 separately for each conformation of the unionized form. Table S6 also contains the values of the distance between the position of the nitrogen atom and the plane P_{CCH} (d). We used this structural parameter to characterize the pyramidality of the (H)C-NH-C_{Ar} fragment in the unionized conformer. Note also that ΔH^0 and ΔS^0 for the transformation between the two forms (UIF ↔ ZIF) have the same sign, *i.e.*, this transformation is reversible.

As can be seen from Table S6, our results fully support the assumption that the stabilization of the unionized form in the case of aromatic substituent is due to the presence of (het)aryl π-electronic system capable of involving the nitrogen lone pair into the conjugation. The flatter the (H)C-NH-C_{Ar} fragment (*i.e.*, the higher the p-character of the nitrogen lone pair) and the larger the π-electronic system of the substituent, the more efficient is the conjugation of the nitrogen lone pair with the (het)aryl π-electronic system and the more stable is the unionized form compared to the zwitterionic one (the more positive is the ΔG^0 value). This trend is observed for all compounds within any series associated with a given conformation of the unionized form. For example, the unionized conformers of **2a** have the least planar (H)C-NH-C_{Ar} fragment and the substituent offers simply a benzene ring. As a result, we got the smallest ΔG^0 values for this compound. In the case of **2d** or **2e**, the substituent has a benzene ring with two (**2d**) or one (**2e**) $COOCH_3$ group(s) capable of participating in the conjugation. For these compounds, we got an almost flat (H)C-NH-C_{Ar} fragment in all unionized conformers. The ΔG^0 values are comparable, but they are always more positive for **2d** because the substituent in this compound has a benzene π-electronic system enlarged by two $COOCH_3$ groups. For **2b**, we got intermediate values of d, but the ΔG^0 values are substantially more positive than those for **2a** and are close to the ΔG^0 values for **2d** and **2e** because the substituent offers an extended (polycyclic) π-electronic system.

In the absence of conjugation, the unionized form is destabilized, and the zwitterionic form is more stable (see Table S8). Note that the more polar solvent increases the stability of the charge-separated (zwitterionic) state. Note also that the influence of specific solvation effects is not taken into account in our calculations. Thus, the ΔG^0 value for **1** is in fact more negative (*i.e.*, the equilibrium for the UIF ↔ ZIF transformation is shifted towards the zwitterionic form, especially in the case of more polar solvent).

Table S1. Molecular structures of various unionized conformers and the corresponding zwitterionic counterparts of α-diphenylphosphino-*N*-(*p*-tolyl)glycine (**2a**).

	UIF	ZIF
I-a	G^0 = -1358.968260 a.u. 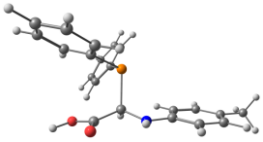	G^0 = -1358.956965 a.u. 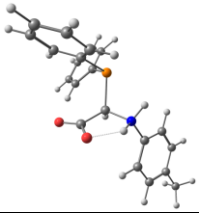
I-b	G^0 = -1358.968627 a.u. 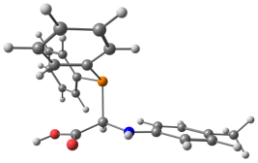	G^0 = -1358.956460 a.u. 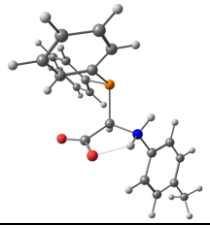
IIA-a	G^0 = -1358.970415 a.u. 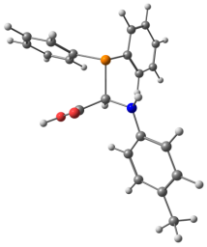	G^0 = -1358.956965 a.u. 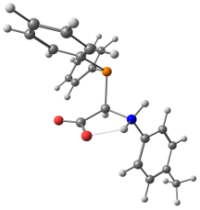
IIA-b	G^0 = -1358.966679 a.u. 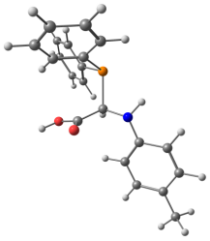	G^0 = -1358.956460 a.u. 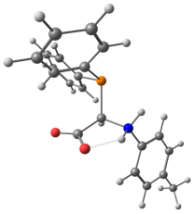
IIB-a	G^0 = -1358.969591 a.u. 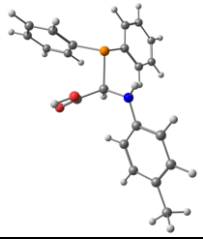	G^0 = -1358.956965 a.u. 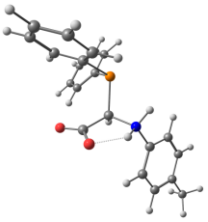
IIB-b	G^0 = -1358.96606 a.u. 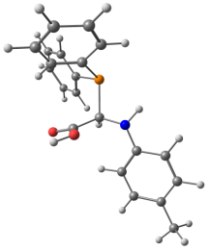	G^0 = -1358.956460 a.u. 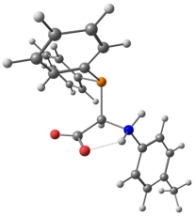

Table S2. Molecular structures of various unionized conformers and the corresponding zwitterionic counterparts of α-diphenylphosphino-*N*-(quinolin-3-yl)glycine (**2b**).

	UIF	ZIF
I-a	G^0 = -1489.373761 a.u. 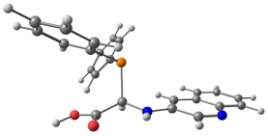	G^0 = -1489.356952 a.u. 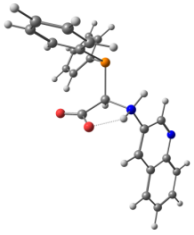
I-b	G^0 = -1489.3740449 a.u. 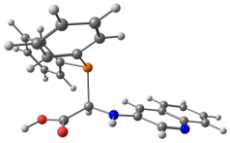	G^0 = -1489.354940 a.u. 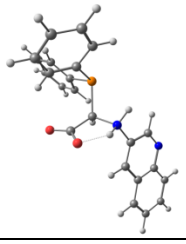
IIA-a	G^0 = -1489.375777 a.u. 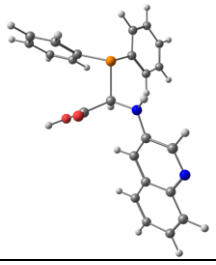	G^0 = -1489.356952 a.u. 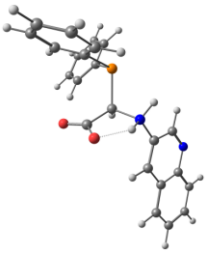
IIA-b	G^0 = -1489.372526 a.u. 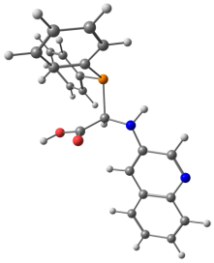	G^0 = -1489.354940 a.u. 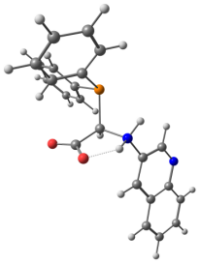
IIB-a	G^0 = -1489.375786 a.u. 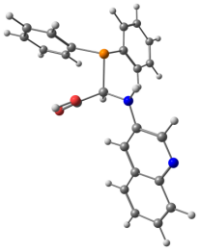	G^0 = -1489.356952 a.u. 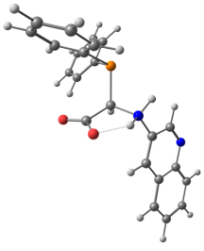
IIB-b	G^0 = -1489.371493 a.u. 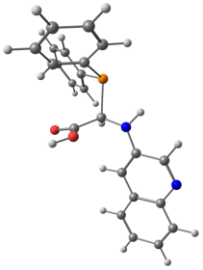	G^0 = -1489.354940 a.u. 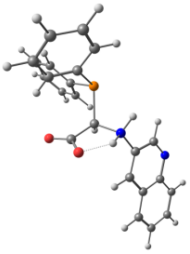

Table S3. Molecular structures of various unionized conformers and the corresponding zwitterionic counterparts of α-diphenylphosphino-*N*-(pyrazin-2-yl)glycine (**2c**).

	UIF	ZIF[(a)]
I-a	G^0 = -1351.780470 a.u. 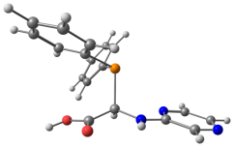	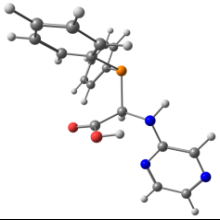
I-b	G^0 = -1351.781369 a.u. 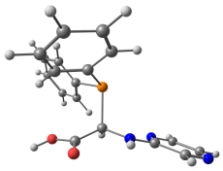	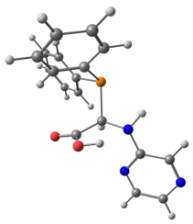
IIA-a	G^0 = -1351.78943 a.u. 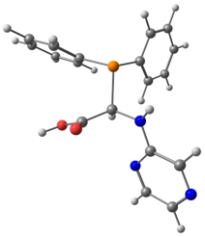	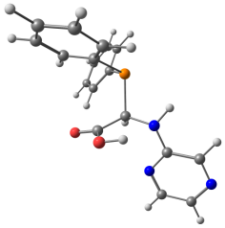
IIA-b	n/a	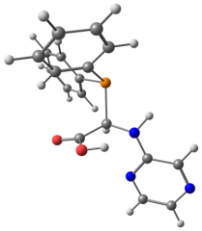
IIB-a	G^0 = -1351.781564 a.u. 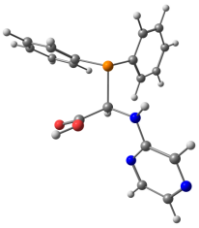	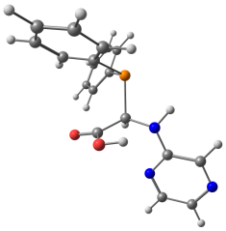
IIB-b	G^0 = -1351.778944 a.u. 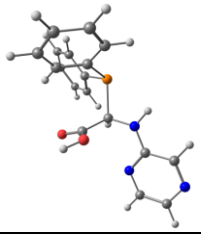	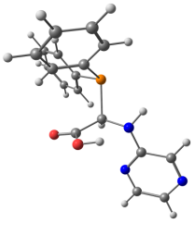

[(a)] Geometry optimizations converge to unionized structures. However, the required conformations of the zwitterionic form may exist due to the specific interactions with the solvent molecules.

Table S4. Molecular structures of various unionized conformers and the corresponding zwitterionic counterparts of α-diphenylphosphino-*N*-[2,5-bis(methoxycarbonyl)phenyl]glycine (**2d**).

	UIF	ZIF
I-a	G^0 = -1775.544733 a.u. 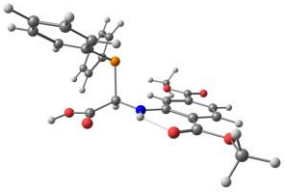	G^0 = -1775.524324 a.u. 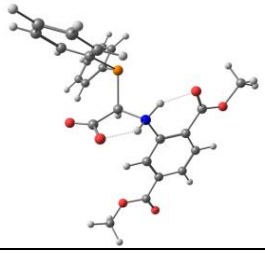
I-b	G^0 = -1775.544402 a.u. 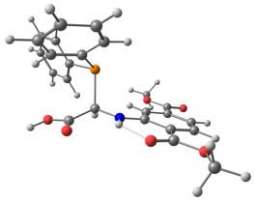	G^0 = -1775.523866 a.u. 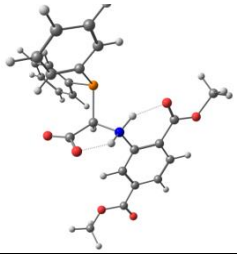
IIA-a	G^0 = -1775.544970 a.u. 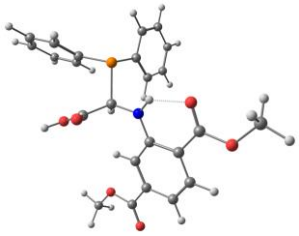	G^0 = -1775.524324 a.u. 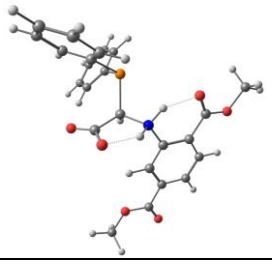
IIA-b	G^0 = -1775.542431 a.u. 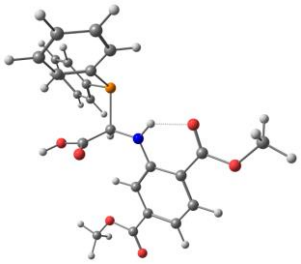	G^0 = -1775.523866 a.u. 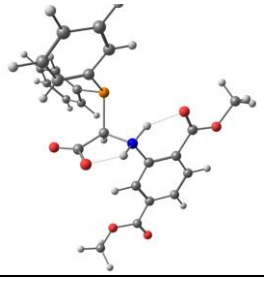
IIB-a	G^0 = -1775.544343 a.u. 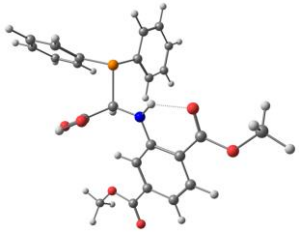	G^0 = -1775.524324 a.u. 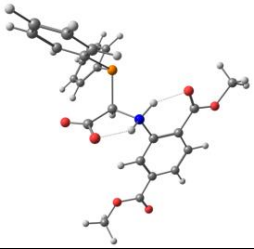
IIB-b	G^0 = -1775.541226 a.u. 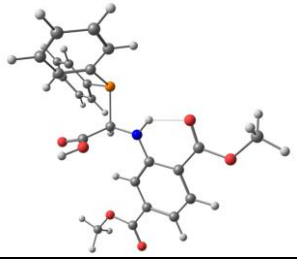	G^0 = -1775.523866 a.u. 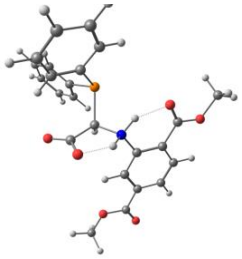

Table S5. Molecular structures of various unionized conformers and the corresponding zwitterionic counterparts of α-diphenylphosphino-*N*-(2-methoxycarbonylphenyl)glycine (**2e**).

	UIF	ZIF
I-a	G^0 = -1547.605051 a.u. 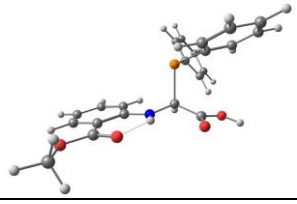	G^0 = -1547.586810 a.u. 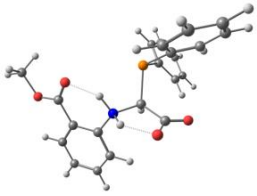
I-b	G^0 = -1547.604037 a.u. 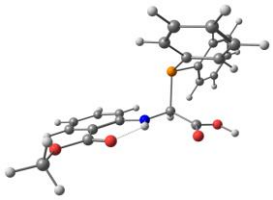	G^0 = -1547.585680 a.u. 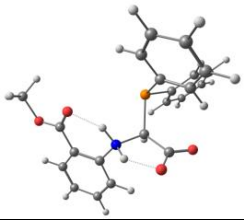
IIA-a	G^0 = -1547.605692 a.u. 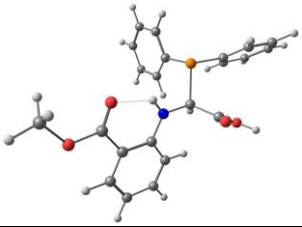	G^0 = -1547.586810 a.u. 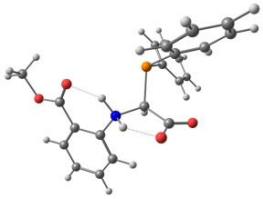
IIA-b	G^0 = -1547.603161 a.u. 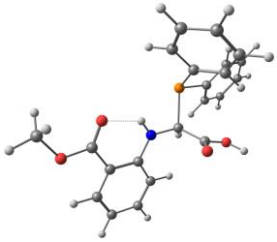	G^0 = -1547.585680 a.u. 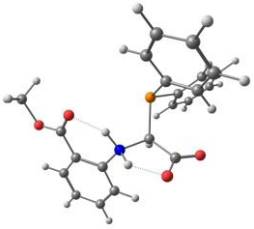
IIB-a	G^0 = -1547.605604 a.u. 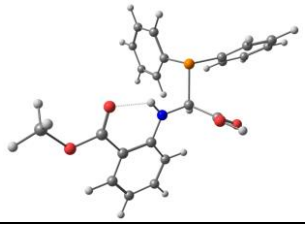	G^0 = -1547.586810 a.u. 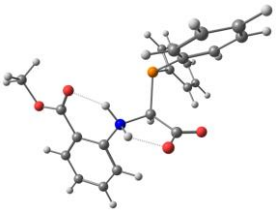
IIB-b	G^0 = -1547.602697 a.u. 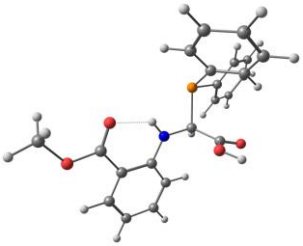	G^0 = -1547.585680 a.u. 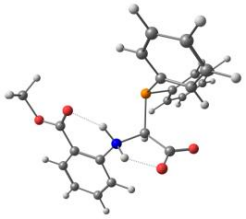

Table S6. The computed values of the Gibbs free energies of the unionized and zwitterionic forms (G^0_{UIF} and G^0_{ZIF}) and their difference (ΔG^0) in methanol (the unionized conformer found in the solid state is marked in bold).

	UIF			ZIF	$\Delta G^0 = G^0_{ZIF} - G^0_{UIF}$
№	conf.	d (Å)	G^0 (a.u.)	G^0 (a.u.)	(kcal/mol)
2a	I-a	0.170	-1358.968260	-1358.956965	7.09
2b		**0.112**	**-1489.373761**	-1489.356952	10.55
2c		0.052	-1351.780470	n/a	n/a
2d		**0.053**	**-1775.544733**	-1775.524324	12.81
2e		0.062	-1547.605051	-1547.586810	11.45
2a	I-b	0.098	-1358.968627	-1358.956460	7.63
2b		0.036	-1489.374049	-1489.354940	11.99
2c		0.018	-1351.781369	n/a	n/a
2d		0.011	-1775.544400	-1775.523866	12.89
2e		**0.021**	**-1547.604037**	-1547.585680	11.52
2a	IIA-a	**0.225**	**-1358.970415**	-1358.956965	8.44
2b		0.194	-1489.375777	-1489.356952	11.81
2c		0.145	-1351.781943	n/a	n/a
2d		0.082	-1775.544970	-1775.524324	12.96
2e		0.081	-1547.605692	-1547.586810	11.85
2a	IIA-b	0.204	-1358.966679	-1358.956460	6.41
2b		0.148	-1489.372526	-1489.354940	11.04
2c		n/a	n/a	n/a	n/a
2d		0.024	-1775.542431	-1775.523866	11.65
2e		0.082	-1547.603191	-1547.585680	10.99
2a	IIB-a	0.212	-1358.969591	-1358.956965	7.92
2b		0.178	-1489.375786	-1489.356952	11.82
2c		0.124	-1351.781564	n/a	n/a
2d		0.070	-1775.544343	-1775.524324	12.56
2e		0.075	-1547.605604	-1547.586810	11.79
2a	IIB-b	0.208	-1358.966006	-1358.956460	5.99
2b		0.145	-1489.371493	-1489.354940	10.39
2c		**0.049**	**-1351.778944**	n/a	n/a
2d		0.017	-1775.541226	-1775.523866	10.89
2e		0.044	-1547.602697	-1547.585680	10.68

Table S7. Molecular structures of the unionized and zwitterionic forms of α-diphenylphosphino-*N*-(*tert*-butyl)glycine (**1**).

№	UIF	ZIF
1	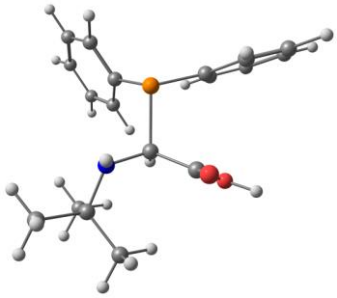	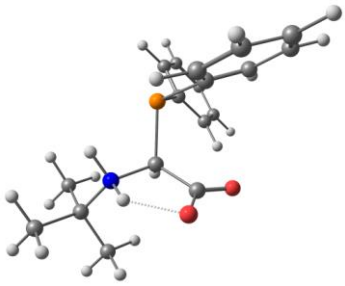

Table S8. The computed values of the Gibbs free energies of the unionized and zwitterionic forms (G^0_{UIF} and G^0_{ZIF}) and their difference (ΔG^0) in methanol and diethylether.

№	solvation model	solvent	UIF G^0 (a.u.)	ZIF G^0 (a.u.)	$\Delta G^0 = G^0_{ZIF} - G^0_{UIF}$ (kcal mol^{-1})
1	SCRF	MeOH	-1245.802397	-1245.805371	-1.87
		Et_2O	-1245.798311	-1245.794752	2.23
	SMD	MeOH	-1245.819160	-1245.827952	-5.52
		Et_2O	-1245.814021	-1245.812351	1.05

References

S1. J. Heinicke, N. Peulecke and P. G. Jones, *Chem. Commun.*, 2005, 262.

S2. J. Lach, C.-Y. Guo, M. K. Kindermann, P. G. Jones and J. Heinicke, *Eur. J. Org. Chem.*, 2010, 1176.

S3. J. Lach, N. Peulecke, M. K. Kindermann, G. J. Palm, M. Kockerling and J. W. Heinicke, *Tetrahedron*, 2015, **71**, 4933.

S4. O. S. Soficheva, G. E. Bekmukhamedov, A. B. Dobrynin, J. W. Heinicke, O. G. Sinyashin and D. G. Yakhvarov, *Mendeleev Commun*., 2019, **29**, 575.

S5. O. S. Soficheva, Yu. A. Kislitsyn, A. A. Nesterova, A. B. Dobrynin and D. G. Yakhvarov, *Russ. J. Electrochem.*, 2020, **56**, 431 (*Elektrokhimiya*, 2020, **56**, 456).

S6. *APEX2, Version 2.1, SAINTPlus, Data Reduction and Correction Program, Version 7.31A, Bruker Advanced X-ray Solutions*, Bruker AXS, Madison, WI, USA, 2006.

S7. G. M. Sheldrik, *SADABS, Program for Empirical X-ray Absorption Correction*, Bruker-Nonius, 1990–2004.

S8. G. M. Sheldrick, *Acta Crystallogr*., 2015, **C71**, 3.

S9. L. J. Farrugia, *J. Appl. Crystallogr.*, 1999, **32,** 837.

S10. A. L. Spek, *Acta Crystallogr.*, 2009, **D65,** 148.

S11. C. F. Macrae, I. J. Bruno, J. A. Chisholm, P. R. Edgington, P. McCabe, E. Pidcock, L. Rodriguez-Monge, R. Taylor, J. van de Streek and P. A. Wood, *J. Appl. Crystallogr.*, 2008, **41**, 466.

S12. M. J. Frisch, G. W. Trucks, H. B. Schlegel, G. E. Scuseria, M. A. Robb, J. R. Cheeseman, G. Scalmani, V. Barone, B. Mennucci, G. A. Petersson, H. Nakatsuji, M. Caricato, X. Li, H. P. Hratchian, A. F. Izmaylov, J. Bloino, G. Zheng, J. L. Sonnenberg, M. Hada, M. Ehara, K. Toyota, R. Fukuda, J. Hasegawa, M. Ishida, T. Nakajima, Y. Honda, O. Kitao, H. Nakai, T. Vreven, J. A. Montgomery, Jr., J. E. Peralta, F. Ogliaro, M. Bearpark, J. J. Heyd, E. Brothers, K. N. Kudin, V. N. Staroverov, R. Kobayashi, J. Normand, K. Raghavachari, A. Rendell, J. C. Burant, S. S. Iyengar, J. Tomasi, M. Cossi, N. Rega, J. M. Millam, M. Klene, J. E. Knox, J. B. Cross, V. Bakken, C. Adamo, J. Jaramillo, R. Gomperts, R. E. Stratmann, O. Yazyev, A. J. Austin, R. Cammi, C. Pomelli, J. W. Ochterski, R. L. Martin, K. Morokuma, V. G. Zakrzewski, G. A. Voth, P. Salvador, J. J. Dannenberg, S. Dapprich, A. D. Daniels, Ö. Farkas, J. B. Foresman, J. V. Ortiz, J. Cioslowski and D. J. Fox, *Gaussian 09, Revision D.01*, Gaussian, Wallingford, CT, 2013.